論文 / 著書情報
Article / Book Information

Title	Experimental investigation of moisture penetration in adhesive layers under varying bonding conditions using near-infrared spectroscopy
Authors	Jin Woo Han, Yu Sekiguchi, Kazumasa Shimamoto, Haruhisa Akiyama, Chiaki Sato
Citation	International Journal of Adhesion and Adhesives, Vol. 134, , 103792
Pub. date	2024, 7
DOI	https://dx.doi.org/10.1016/j.ijadhadh.2024.103792

International Journal of Adhesion & Adhesives 134 (2024) 103792

Contents lists available at ScienceDirect

International Journal of Adhesion and Adhesives

journal homepage: www.elsevier.com/locate/ijadhadh

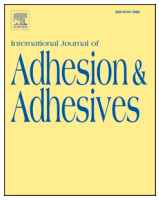

Experimental investigation of moisture penetration in adhesive layers under varying bonding conditions using near-infrared spectroscopy

Jin-Woo Han [a,*], Yu Sekiguchi [b,**], Kazumasa Shimamoto [c], Haruhisa Akiyama [c], Chiaki Sato [b]

[a] Department of Mechanical Engineering, Tokyo Institute of Technology, 4259 Nagatsuta-cho, Midori-ku, Yokohama, 226-8501, Kanagawa, Japan
[b] Institute of Innovative Research, Tokyo Institute of Technology, 4259 Nagatsuta-cho, Midori-ku, Yokohama, 226-8501, Kanagawa, Japan
[c] Nanomaterials Research Institute, National Institute of Advanced Industrial Science and Technology (AIST), 1-1-1 Higashi, Tsukuba, 305-8565, Ibaraki, Japan

ARTICLE INFO

Keywords:
Non-destructive testing
Infrared spectroscopy
Durability
Water resistance
Moisture distribution
Water penetration

ABSTRACT

The mechanical properties of adhesive joints are affected by the moisture content, making it necessary to understand the moisture diffusion behavior in the adhesive layer. The diffusion coefficient of the bulk material is generally used in the numerical calculation of the penetration distance; however, the joint strength often decreases beyond the expected value. Therefore, it is believed that moisture penetrates much faster in the adhesive layer than in the bulk, although there have been no direct observations of this behavior. In this study, the effects of the adhesive thickness and surface wettability of the substrate on moisture penetration into the layer were investigated. Near-infrared spectroscopy was applied to non-destructively reveal the in-plane moisture distribution in the adhesive layer. The moisture distribution in the adhesive layer sandwiched between quartz glasses was monitored for six weeks by immersing it in room-temperature water. Two adhesive layers with different thicknesses (0.3 and 0.1 mm) were prepared, and it was revealed that the thinner the adhesive layer, the faster the moisture diffusion. A numerical analysis based on Fick's law showed that the diffusion coefficient of a 0.1 mm-thick adhesive layer was approximately 1.6 times greater than that of the bulk. In addition, the different surface wettability resulted in a change in the diffusion behavior at the corners of the adhesive layer, although there was little difference in the case of unidirectional penetration.

1. Introduction

The adhesive bonding technology plays a crucial role in various industries, such as aerospace and automotive, owing to its capability in joining dissimilar materials [1]. Understanding the factors affecting the mechanical properties of adhesive joints is essential to ensure their reliability and performance. Moisture has long been known to influence the behavior of adhesive joints [2,3]. When adhesives are exposed to a humid environment, the increased moisture content can lead to a deterioration in their mechanical properties [4,5], and the moisture absorbed near the interface reduces their interfacial strength [6,7]. Especially, when metallic substrates are used as the adherend, moisture diffusion near the interface not only degrades the adhesives but also corrodes the substrate, having a detrimental effect on the adhesive joint [8].

In adhesive bonding, because the adhesive layer is sandwiched between adherends, moisture can diffuse from the sides of the adhesive layer and disperse within the adhesive layer. While the moisture diffusion into the adhesive layer has been conventionally predicted using Fickian diffusion [9], some studies have suggested the possibility that diffusion near the interface may be faster than the Fickian diffusion into the adhesive layer [10–12]. Zanni-Deffarges et al. [10] proposed the concept of capillary diffusion and demonstrated the possibility of rapid diffusion near the interface, which can influence the overall diffusion behavior of the entire adhesive layer. Although direct measurements of the moisture distribution within adhesive layers have been made using non-destructive methods, such as Fourier transform infrared (FTIR) transmission microscopy and near-infrared spectroscopy (NIRS) [12,13], only a limited number of such cases have been reported. The actual state of moisture penetration into the adhesive layer remains unclear.

The diffusion coefficient of an adhesive is a material property that does not vary with the bonding conditions. If a change in the moisture distribution is observed under varying conditions, the change is due to an effect other than the diffusion coefficient of the material itself. The

* Corresponding author.
** Corresponding author.
E-mail addresses: han.j.aj@m.titech.ac.jp (J.-W. Han), sekiguchi.y.aa@m.titech.ac.jp (Y. Sekiguchi).

https://doi.org/10.1016/j.ijadhadh.2024.103792
Received 29 June 2024; Accepted 15 July 2024
Available online 20 July 2024

thinner the adhesive layer, the greater the effect of moisture ingress at the interface on the entire adhesive layer. When the surface wettability of an adherend varies, moisture intrusion into the interface may affect the moisture distribution.

In this study, we measured the moisture distribution in an adhesive layer composed of epoxy by varying the thickness of the adhesive layer and the surface wettability of the substrate to investigate the influence of moisture diffusion near the interface on the overall moisture diffusion in the adhesive layer. NIRS was applied for the water content analysis. Quartz glass was used as the substrate given that it allows for the transmission of NIR rays. Specimens with two different thicknesses and under three different surface conditions were prepared.

2. Experimental

2.1. Materials and specimens

2.1.1. Adhesive

A thermoset adhesive was used in this study. Table 1 lists its composition. This adhesive has simple components: a bisphenol A epoxy resin and a curing agent. The use of simple materials is known to help prevent complex diffusion phenomena within an adhesive, including a reduction in the free volume for moisture diffusion and moisture accumulation at the interface between the resin and filler [14]. The curing temperature was set to 180 °C for 30 min to ensure sufficient adhesive curing.

2.1.2. Substrates

A quartz glass plate with a thickness of 1 mm and a width/length of 25 mm was used. Quartz glass allows the transmission of NIR rays and does not absorb moisture. Therefore, the moisture within the adhesive layer can be investigated using NIRS [13].

Three different surface treatments were applied to investigate the effects of wettability on the moisture diffusion near the interface. In the first treatment, the surface was degreased with acetone prior to bonding. In the second treatment, flame treatment was employed to render the substrate surface hydrophilic. Flame treatment has been utilized as a method to increase surface energy and enhance hydrophilicity by processes such as cleaning contaminants and modifying surface chemistry [15,16]. In the third treatment, to render the substrate surface hydrophobic, a fluoropolymer (CYTOP, AGC Co. Ltd., Tokyo, Japan) was spin-coated onto a quartz glass plate at 1000 rpm for 30 s and then cured at 80 °C for 1 h and 200 °C for 1 h. Fig. 1 shows the contact angles on the substrates subjected to the three different surface treatments.

2.1.3. Specimens

The types of specimens used in this study, along with their adhesive thickness and surface treatment, are listed in Table 2. Two types of specimens were prepared to investigate the moisture diffusion: open-face and closed specimens. The open-face specimens were used for the gravimetric method and NIR spectral analysis given their rapid and uniform moisture diffusion into the adhesive–substrate interface. To adjust the adhesive thickness, a polytetrafluoroethylene tape with a thickness of 0.3 mm and a width of 1 mm was attached to the four sides of the quartz glass plate, resulting in an adhesive area of 529 mm^2, as shown in Fig. 2a. The closed specimens were used to measure the moisture distribution. In this case, only the edges of the adhesive layer were exposed, resulting in a moisture distribution in the adhesive layer.

Table 1
Chemical composition of the adhesive used in this study.

Material	Mass (%)
Bisphenol A epoxy resin	88
Dicyandiamide	10
3-(3,4-dichlorophenyl)-1,1′-dimethylurea	2

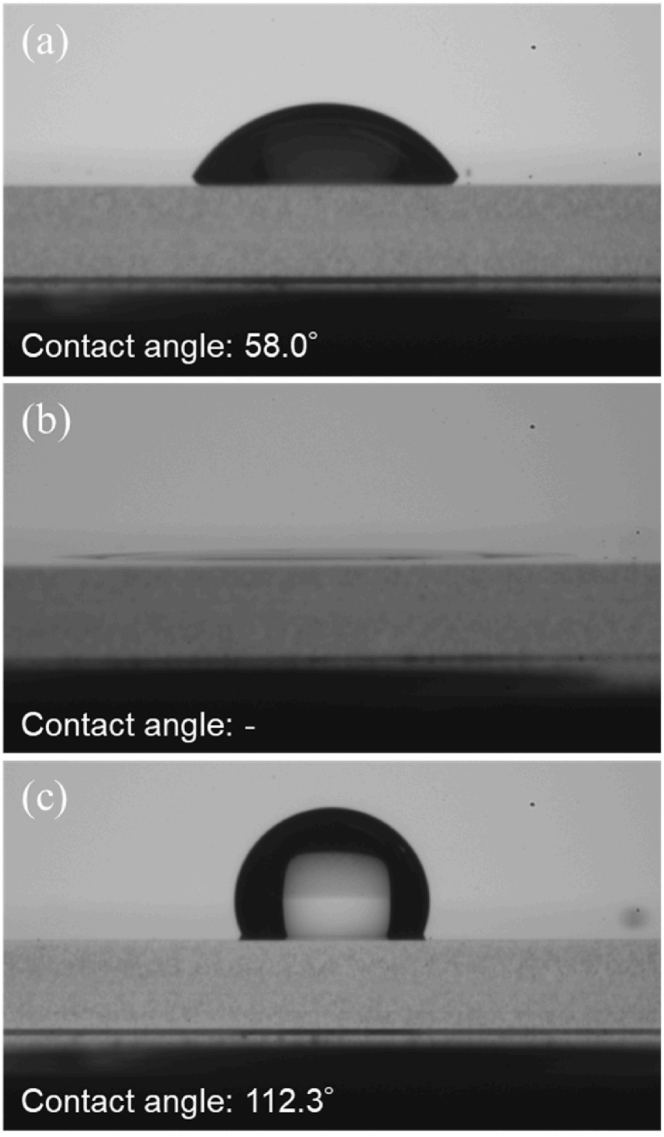

Fig. 1. Water contact angles on quartz glass plates subjected to different surface treatments: (a) acetone degreasing, (b) hydrophilic treatment, and (c) hydrophobic treatment.

Table 2
Specimen types and surface treatments used in this study.

Specimen type	Adhesive thickness (mm)	Surface treatment
Open-face	0.3	Acetone degrease
Closed	0.1	Acetone degrease
		Flame treatment (hydrophilic)
		Fluoropolymer modified (hydrophobic)
	0.3	Acetone degrease

To control the adhesive thickness, glass beads of the same diameter as the adhesive thickness were inserted. The adhesive area was the same as that of the quartz glass plate, 625 mm^2, as shown in Fig. 2b.

The adhesive thicknesses of the closed specimens were set to 0.1 and 0.3 mm to investigate the effect of adhesive thickness on the moisture diffusion in the adhesive layer. Only the acetone-degreased substrate was used in both the open-face and closed specimens with an adhesive thickness of 0.3 mm. Three types of substrates–acetone degreased, hydrophilic treated, and hydrophobic treated–were used for the closed

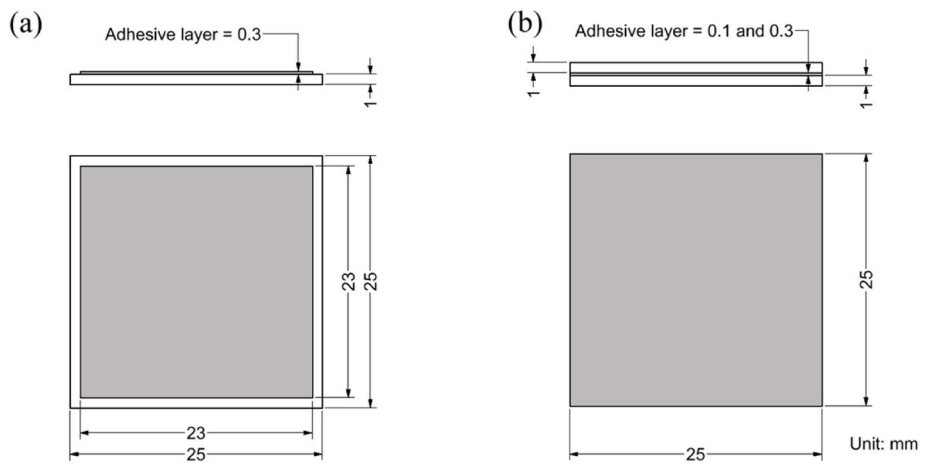

Fig. 2. Schematics of (a) open-face and (b) closed specimens.

specimen with an adhesive thickness of 0.1 mm to investigate the effect of surface conditions on moisture diffusion near the interface. Specimens degreased with acetone were used to investigate the effect of the adhesive thickness, whereas hydrophilic- and hydrophobic-treated specimens were used to investigate the effect of surface conditions on moisture diffusion in the adhesive layer.

To evaluate the change in the specimen conditions, the results of closed specimens composed of an A6061-T6 aluminum alloy plate and a quartz glass plate in Ref. [13] were used for the comparison. The dimensions of the aluminum alloy plate for the lower substrate were 3 mm in thickness, 25 mm in width, and 100 mm in length, and the same quartz glass plate as in this study was used for the upper substrate. Thus, the bonded area was the same. The aluminum alloy plate was initially degreased with acetone, then immersed in a 60 °C alkaline solution for 30 s, followed by washing with purified water and drying. Afterward, it was immersed in an acidic solution at 60 °C for 30 s. To bond the aforementioned substrates, an adhesive based on bisphenol A epoxy resin as the base resin was used. Dicyandiamide was used as a curing agent, and carboxyl-terminated butadiene acrylonitrile rubber was used as a strengthener. Several other additives were also used. Curing was conducted at 180 °C for 60 min.

2.2. Experimental setup

The measurement setup shown in Fig. 3 has been well-established, as described in a previous study [13]. The NIR spectra were acquired in reflection mode using a NIR spectrometer (NIRONE S2.2, Spectral Engines, Steinbach, Germany) from an average of 100 values in the thickness direction. Given that both the substrates were quartz glass plates that allow NIR-ray transmission, a gold mirror reflecting over 98 % of the NIR rays was placed under the specimen.

All the scans were performed under laboratory conditions. The measured spectral range was 1750–2150 nm with a wavelength interval of 1 nm for the open-face specimens and 5 nm for the closed ones. Fig. 4 shows the scanning area. For the open-face specimens, 11 points were measured along the centerline of the specimen with a scanning pitch of 0.5 mm. In the case of the closed specimens, considering symmetry, only a quarter of the specimen surface was measured. The scanning pitch was 0.5 mm, and a total of 625 points were scanned. The origin coordinates were set at the lower-left corner of the specimen.

2.3. Experimental procedure

In this study, the immersion temperature was set to room temperature (approximately 23 °C). The specimens were placed in plastic bags containing purified water. Fig. 5 shows the entire procedure. The immersed specimens were removed from the water for scanning. After wiping the surface, we measured the moisture content using the open-face specimen. The moisture content was calculated as follows:

$$m_t\,[\%] = \frac{M_t - M_0}{M_0} \times 100, \tag{1}$$

where m_t is the moisture content. M_0 and M_t are the masses of the adhesives before and after immersion, respectively. The mass of the quartz

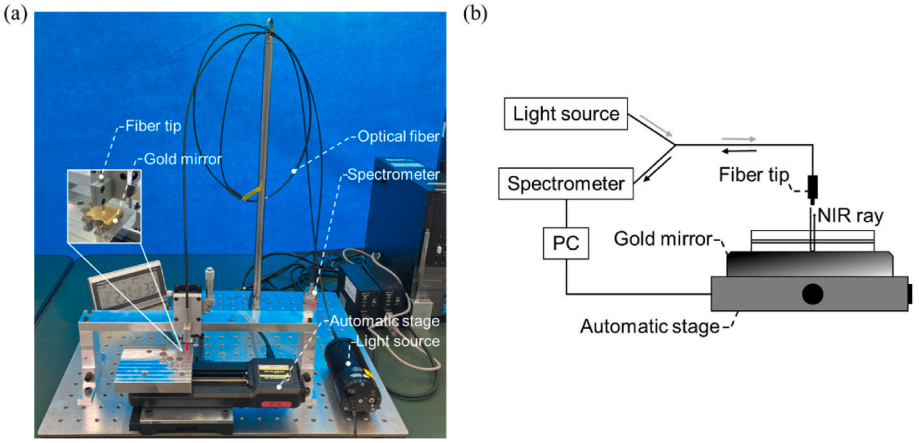

Fig. 3. (a) Image of the NIRS measurement setup, and (b) schematic of the operation of the instrument.

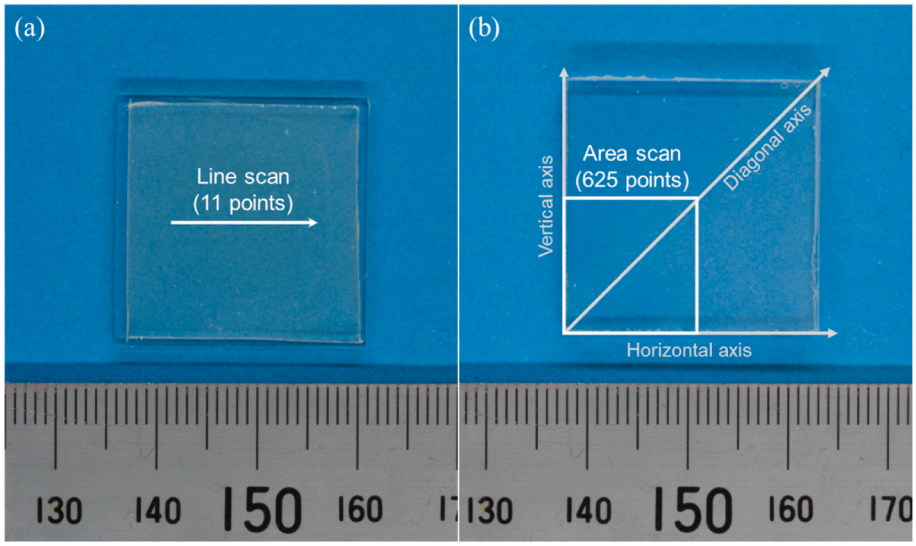

Fig. 4. Scanning areas of (a) open-face specimen and (b) closed specimen.

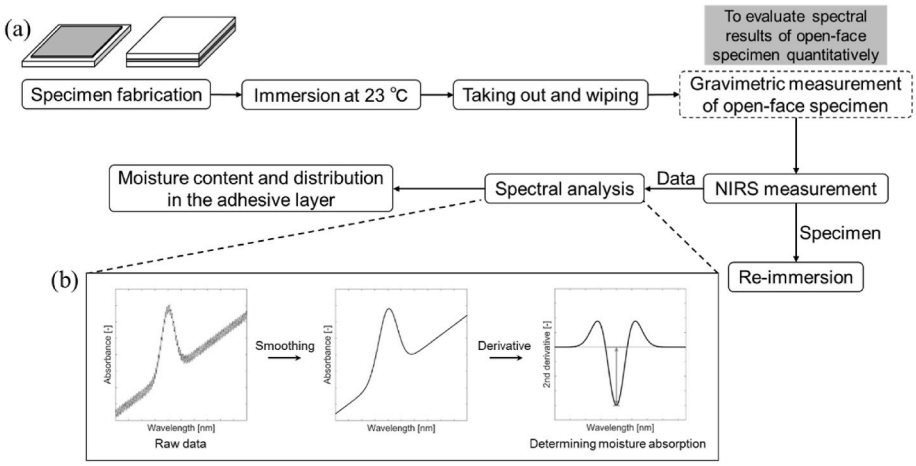

Fig. 5. Illustration of (a) experimental procedure from specimen fabrication to data analysis and (b) spectral analysis to determine moisture absorption.

glass, which was measured before specimen fabrication, was subtracted from the total mass of the open-face specimen to calculate the mass of the adhesive. The specimen was weighed using an electronic balance with a resolution of 0.1 mg (VIBARA HTR-220, Shinko Denshi, Tokyo, Japan). After the gravimetric measurements, the specimens were measured using an NIRS measurement system. For the closed specimens, NIRS measurements were performed directly without gravimetric measurements. After the NIRS measurements, the specimens were re-immersed in purified water, and the acquired data were processed through a spectral analysis.

2.4. Spectral analysis

The intensity values of the reflectance spectra were converted into absorbance values as follows:

$$A = -\log_{10}\left(\frac{I}{I_0}\right), \tag{2}$$

where, A is the absorbance, I is the measured intensity, and I_0 is the background intensity. Before each measurement, a background spectrum was obtained using a specimen featuring an air gap of the same thickness between the quartz glass plates instead of the adhesive layer.

The absorbance values were subjected to smoothing using a 3rd-order Savitzky-Golay filter with filter windows of 150 for open-face specimens and 15 for closed specimens before second-derivative processing. Filtering was performed using the open-source preprocessing module Nippy by Python 3.10 [17]. In this study, the second-derivative method (SDM) was employed to determine the moisture absorption of the layer from the NIR spectra. The second-derivative technique in the NIRS data analysis has the advantage of improving the quantification accuracy by eliminating baseline shifts and rotations in the spectrum [13,18]. Because the peaks in the absorbance spectrum correspond to the negative peaks in the second-derivative spectrum, the absolute value of the second-derivative peak was considered the moisture absorption value. For the open-face specimens, the moisture absorption was calculated as the average of the absorption intensities at 11 points. For the closed specimens, the moisture absorption was plotted at each coordinate to visualize the moisture distribution.

3. Results and discussion

3.1. Quantitative evaluation of moisture absorption of open-face specimen

3.1.1. Gravimetric analysis

Fig. 6 shows the changes in the moisture content of the open-face specimens. The moisture content initially increased rapidly and then

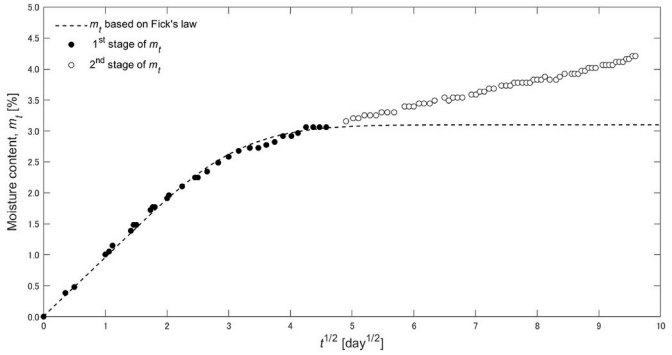

Fig. 6. Changes in the moisture content of open-face specimen during the immersion time.

increased slowly and steadily. In epoxy materials, moisture diffuses in two stages such as a combination of Fickian and non-Fickian diffusion or dual-Fickian diffusion [19,20]. The first stage, Fick's law of diffusion, can be expressed as follows:

$$m_t = m_\infty \left[1 - \sum_{n=0}^{\infty} \left\{ \frac{8}{(2n+1)^2 \pi^2} \right\} \exp\left\{ -D \frac{(2n+1)^2 \pi^2}{4w^2} t \right\} \right], \quad (3)$$

where m_t is the moisture content at an immersion time of t, m_∞ is the saturation moisture content in the first stage, w is the adhesive thickness, and D is the diffusion coefficient. By fitting Eq. (3) to the experimental results, we determined the diffusion coefficient. However, the boundary between the first and second stages of diffusion remained unclear in the experimental results. To address this issue, we focused on the region where the moisture content vs. square root of time data shows a linear starting and reaches a plateau indicative of saturation [21]. This trend was observed between approximately 18 and 46 days after immersion. The time corresponding to the highest coefficient of determination within this range was chosen as the endpoint for the first stage of diffusion, and the diffusion coefficient was calculated accordingly. Table 3 presents the values of the obtained parameters.

3.1.2. Spectral analysis

Fig. 7 shows the changes in the absorbance and second-derivative spectra. In both spectra, the peak in the 1900–1950 nm range varied with the immersion time; this peak originated from the absorption band of the water molecules. Fig. 8 shows the changes in the peak values over the immersion time. The increments in the peak intensity were defined as changes from the peak intensity at an immersion time of 0 d. For the second-derivative spectra, the absolute values were used because the peaks appeared in the negative direction. Similar to the moisture content changes observed in the gravimetric analysis, the peak intensity change exhibited a rapid increase during the initial period. Fig. 9 shows a comparison between the moisture content from gravimetric changes and the peak intensity from absorbance and second-derivative spectra, where the values are normalized to the value observed at the end of the first stage. The coefficient of determination between the moisture content and the peak intensity in the first stage was 0.974 for the absorbance spectra and 0.972 for the second-derivative spectra, showing a linear correlation. However, the difference increased with the immersion time in the second stage. Although the peak intensity increased for both

Table 3
Parameter values of Fick's law of diffusion.

Adhesive thickness (mm)	Saturated moisture content (%)	Diffusion coefficient (mm^2/h)	Coefficient of determination (R^2)
w	m_∞	D	R^2
3.15×10^{-1}	3.10	3.10×10^{-4}	0.995

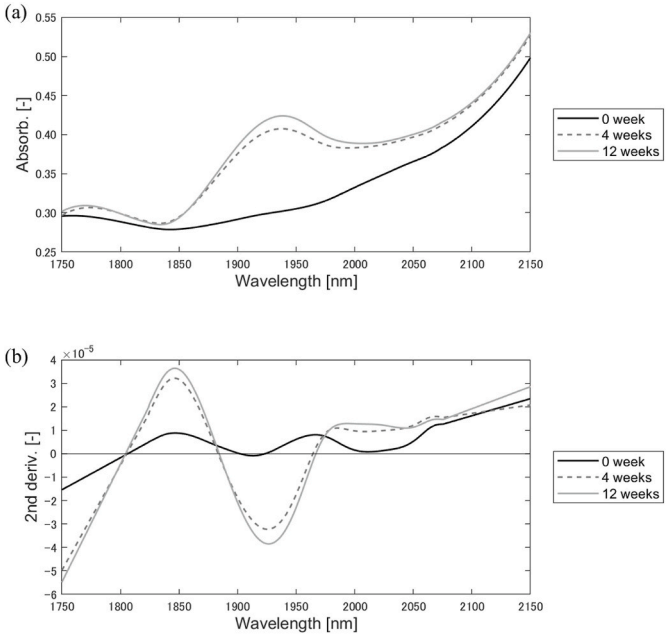

Fig. 7. Spectral changes in the (a) absorbance spectra and (b) second-derivative spectra of the open-face specimen.

absorbance and second-derivative spectra, the increase was smaller than the increase in moisture content. Therefore, the coefficient of determination in the entire range decreased to 0.813 for the absorbance spectra and 0.916 for the second-derivative spectra. In the discussion of moisture distribution, an analysis was performed using the second-derivative spectra, which have less difference concerning the moisture content.

3.2. Evaluation of improved closed specimens

In this study, different adhesive and substrates from the development stage of the NIR monitoring system [13] were used. Because general adhesives contain many additives such as fillers and silica, which complicate the water absorption process, pure materials are recommended for analysis. Furthermore, when the upper and lower substrates are different, different diffusion behaviors may occur at the interface between the respective substrates and the adhesive layer. The complexity of moisture diffusion due to different diffusion behaviors within a specimen can pose significant obstacles to analyzing the effect of adhesive thickness and surface condition on moisture diffusion. Therefore, using the same material on the upper and lower substrates can reduce the complexity of diffusion within the specimen. This facilitates more accurate analysis. Hence, we changed the specimen conditions from those reported in our previous study [13]. Herein, we discuss how the specimen condition changed the moisture distribution in the adhesive layer.

Fig. 10a–c show the results of moisture distribution in the adhesive layer sandwiched between the quartz glass plate and the aluminum alloy. Fig. 10d–f show the results of moisture distribution in the adhesive layer sandwiched between the quartz glass plates. The region ranging from 0 mm to 0.5 mm is represented in black because the scattering of the light at the edges of the specimens prevented the acquisition of accurate moisture absorption data. Each dataset was normalized by taking the maximum value at an immersion time of six weeks for each specimen, and the moisture distribution was plotted. Fig. 11 shows the changes in the moisture detection area with respect to the immersion time.

Numerical simulations were also conducted using the finite element method (FEM). The diffusion process was modeled using Abaqus/CAE 2023 with a square mesh size of 0.125 mm for the 2D analysis. The

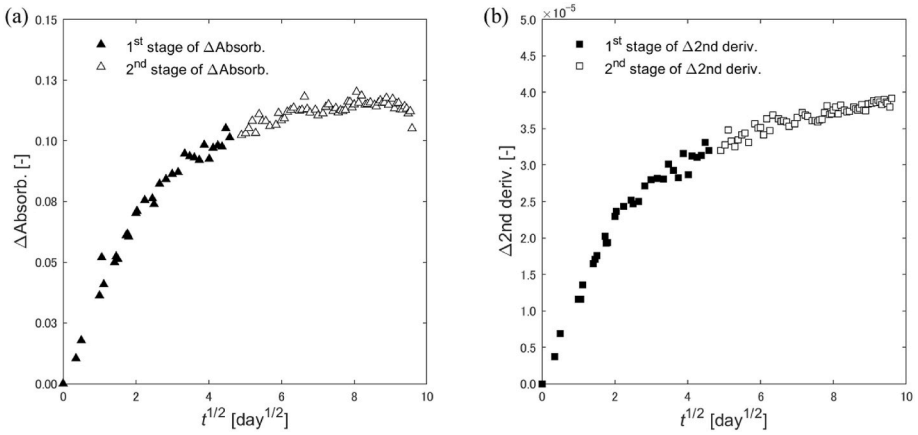

Fig. 8. Changes in the peak intensity of (a) absorbance spectra and (b) second-derivative spectra during the immersion time.

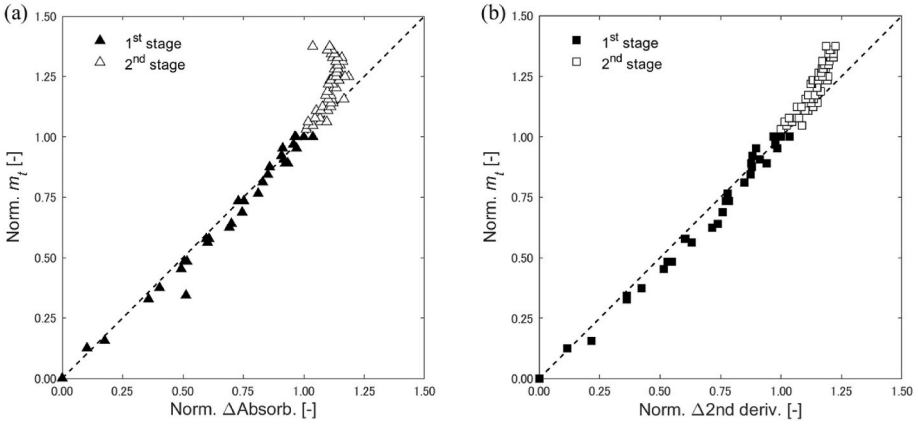

Fig. 9. Comparison between the moisture content and peak intensity in the (a) absorbance spectra and (b) second-derivative spectra.

boundary conditions were given as complete saturation of the water-contacting surface. In the numerical analysis, the diffusion coefficient of the bulk materials was used, and Fick's law of diffusion was assumed, i.e., only the first diffusion stage was considered.

The calculation of the moisture distribution from the side to the center and from the corner to the center of the specimen is shown in Fig. 12. Since the diffusion front from the side is not a perfectly straight line, the average value of the moisture distribution from 7.5 mm to 12.5 mm in both the vertical and horizontal directions was adopted as the moisture distribution distance from the side (Fig. 12a). In the case of from the corner to the center, since there is only one axis present, the moisture distribution was plotted with an axis set in the direction of Fig. 12b.

Fig. 13a shows the moisture content distribution in the direction from the side to the center of the specimens after six weeks of immersion; Fig. 13b shows the moisture content distribution in the direction from the corner to the center (i.e., the diagonal direction). The numerical results were calculated by inputting the diffusion coefficients obtained from the gravimetric measurements of each adhesive; these values were 5.64×10^{-4} mm^2/h for the quartz–aluminum specimen and 3.10×10^{-4} mm^2/h for the quartz–quartz specimens.

Experimental results of the quartz–aluminum specimen showed a different diffusion trend from the numerical results considering Fickian diffusion, particularly in diffusion near the edges. In contrast, experimental results of the quartz-quartz specimen showed relatively good agreement in distribution with Fickian diffusion. When using a metal substrate as an adherend, factors other than the diffusion coefficient of the adhesive itself may affect moisture diffusion in the quartz-aluminum specimen, such as changes in crosslink density near the substrate surface due to the interaction between curing agent and metal oxides [7]. In other words, the quartz–quartz specimen used in this study showed diffusion behavior closer to Fickian diffusion, enabling a more accurate discussion regarding the effects of adhesive thickness and substrate surface conditions on moisture diffusion.

3.3. Factors affecting moisture diffusion in the adhesive layer

3.3.1. Effect of adhesive thickness

Fig. 14a–c show the results of moisture distribution of acetone-degreased specimens with an adhesive thickness of 0.1 mm. At an immersion time of two weeks, a vertical wave-like distribution was observed, whereas a horizontal wave-like distribution was observed at an immersion time of four weeks. The wavelike distributions were alleviated at an immersion time of six weeks. These wavy distributions could have resulted from actual diffusion in this pattern. However, the fact that such a distribution is no longer maintained with increasing immersion time suggests that the results may not reflect actual diffusion. Wavy distributions were not observed in quartz-aluminum and quartz-quartz specimens with an adhesive thickness of 0.3 mm. However, wavy distributions were observed when the adhesive thickness was reduced to 0.1 mm. Therefore, it is conceivable that irradiated NIR rays interfere between the upper and lower substrates when a very small amount of moisture accumulates, leading to the formation of wavy distributions.

Fig. 15a shows the result of moisture content distributions from the side of the specimens after six weeks of immersion; Fig. 15b shows the

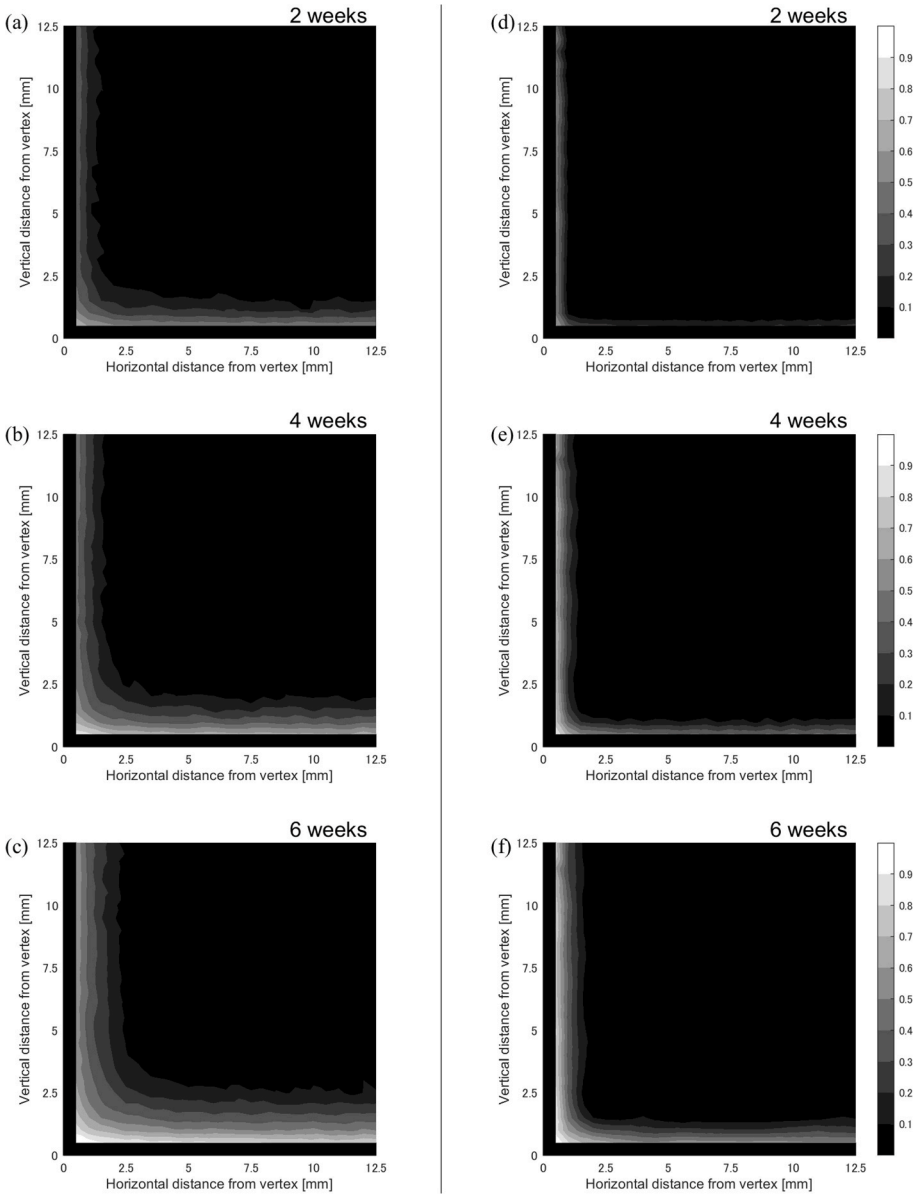

Fig. 10. Moisture distributions in a closed specimen with an adhesive thickness of 0.3 mm determined using the second-derivative method (SDM): (a)–(c) quartz glass–aluminum alloy specimen; (d)–(f) quartz glass–quartz glass specimen.

result from the corner. Comparing the results of the 0.1 mm- and 0.3 mm-thick specimens, we found that the thinner adhesive layer allows for more moisture penetration. The diffusion coefficient of the bulk material was 3.10×10^{-4} mm^2/h, while the results of the 0.1 mm- and 0.3 mm-thick specimens were close to the numerical results with the diffusion coefficient of 5.00×10^{-4} and 4.00×10^{-4} mm^2/h. Hence, it was suggested that the diffusion coefficient of the 0.1 mm-thick adhesive layer was approximately 1.6 times greater than that of the material itself.

Fig. 16 shows a schematic of the moisture distribution in the thickness direction under different adhesive thicknesses. Assuming no specific moisture diffusion occurs near the interface, the in-plane distribution must remain constant, regardless of the adhesive thickness (Fig. 16a). In contrast, it can also be considered that moisture near the interface diffused faster than the center of the adhesive layer, as shown in Fig. 16b [10,11,22]. Such rapid distribution may be attributed to differences in the concentration of curing agent in the thickness direction [23], differences in substrate surface wettability [10], and so forth. These factors could change crosslink density near the interface and affect moisture diffusion near the interface [24]. Furthermore, when glass is used as the substrate, it leads to interfacial failure between glass and adhesive, indicating moisture diffusion near the interface [25,26]. However, detecting small amounts of moisture near the interface using NIRS is challenging due to weak absorbance. Despite this challenge, the experimental results showed that the diffusion coefficients of the adhesive layer, particularly the thinner layer, were greater than those calculated using the gravimetric method. Consequently, the rapid moisture diffusion near the interface would have accelerated the overall moisture diffusion in the adhesive layer as it diffused back towards the dry region, such as the center of the adhesive layer. This is also confirmed by the observation that the moisture distribution is broader when the adhesive thickness is thin.

3.3.2. *Effect of surface condition*

Fig. 14d–f and 14g–i show the results of moisture distribution of the hydrophilic and hydrophobic treated specimens, respectively. Fig. 17 shows the time changes in the moisture detection area after immersion. No significant differences were observed in the in-plane distributions. However, as shown in Fig. 18, the hydrophilic-treated specimen appears

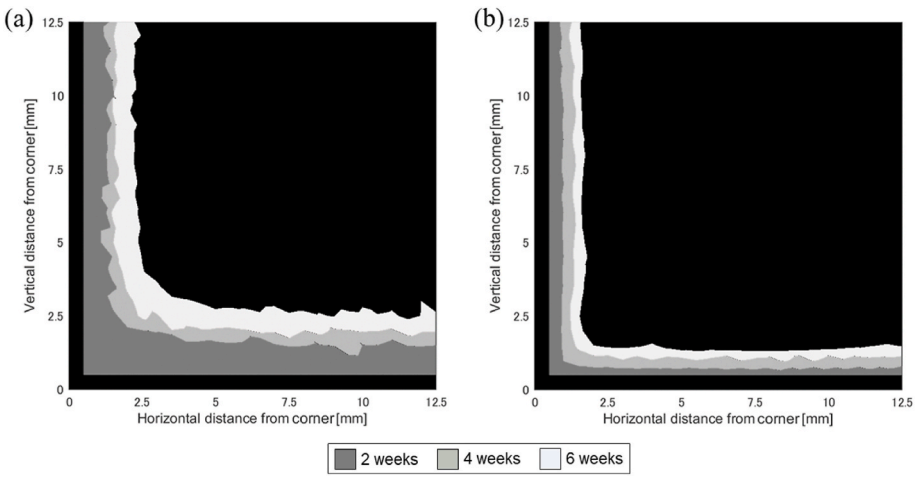

Fig. 11. Changes in the moisture-detected area with respect to the immersion time of (a) quartz glass–aluminum alloy specimen and (b) quartz glass–quartz glass specimen with an adhesive thickness of 0.3 mm.

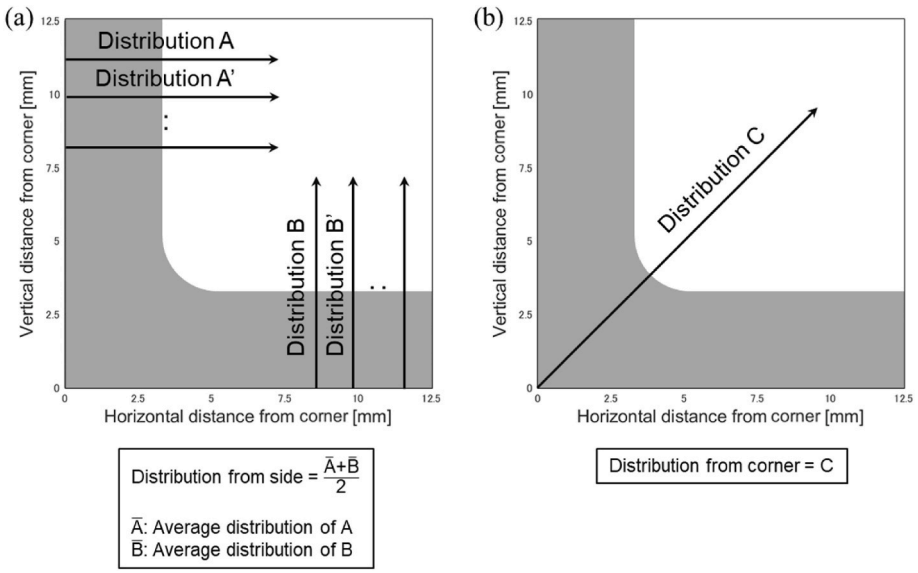

Fig. 12. Schematic of the distances used in the analysis to determine the moisture distribution (a) from side to center and (b) from corner to center.

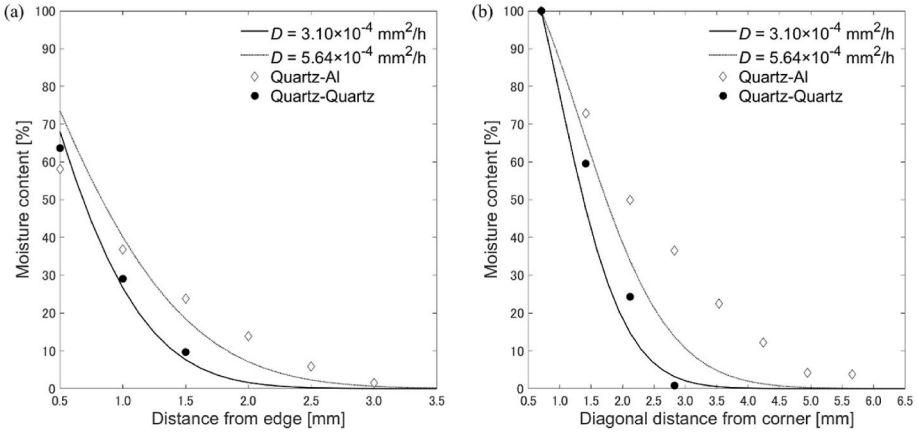

Fig. 13. Moisture content distribution in specimens with different substrates and adhesives at an immersion time of six weeks (a) from the side to the center and (b) from the corner to the center of specimen.

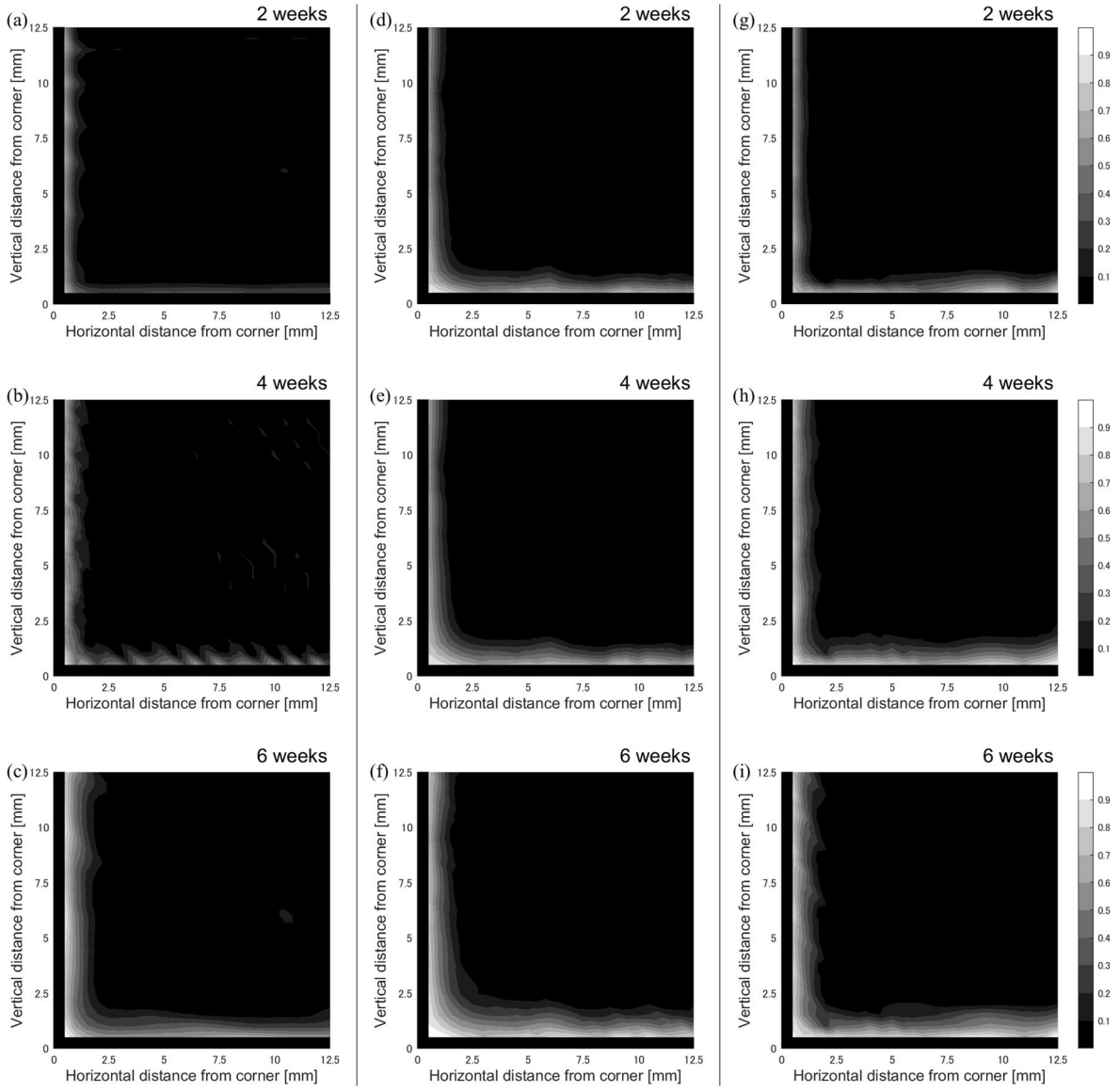

Fig. 14. Moisture distributions of closed specimens with an adhesive thickness of 0.1 mm determined using the second-derivative method (SDM), with the substrates subjected to: (a)–(c) acetone degreasing; (d)–(f) hydrophilic treatment; (g)–(i) hydrophobic treatment.

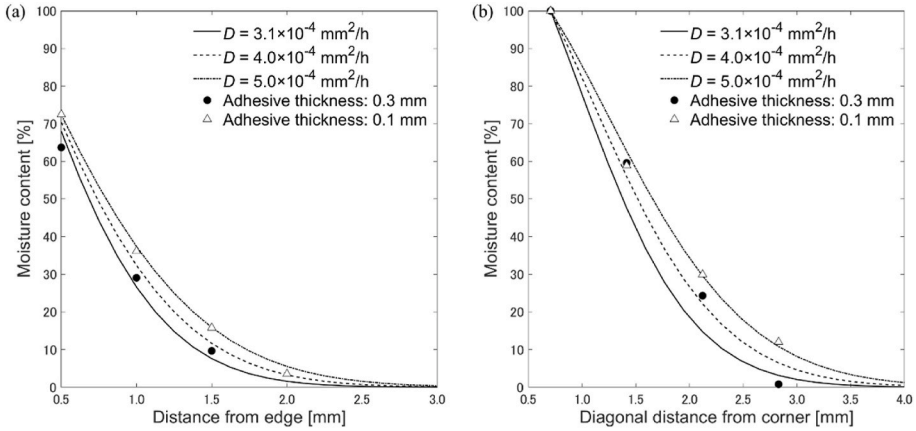

Fig. 15. Moisture content distribution in specimens with different adhesive thicknesses at an immersion time of six weeks (a) from the side to the center and (b) from the corner to the center of the specimen.

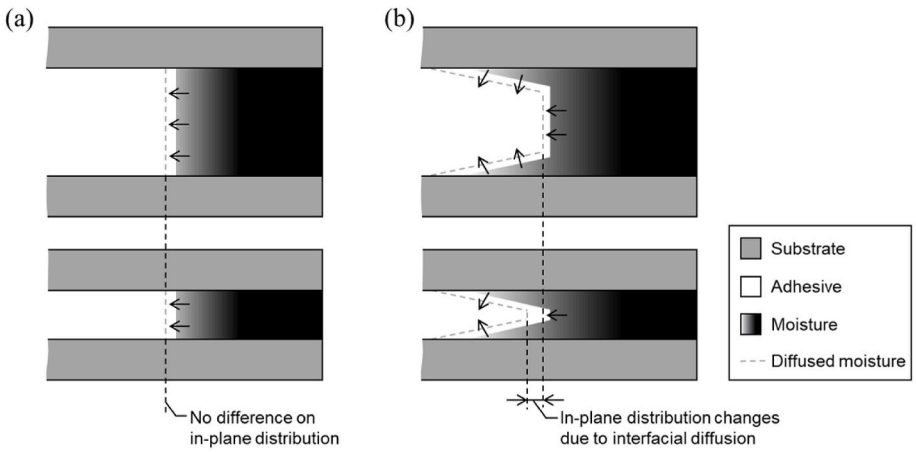

Fig. 16. Schematics of the moisture distribution of the specimens with different adhesive thicknesses in the thickness direction: (a) no diffusion near the interface and (b) diffusion near the interface.

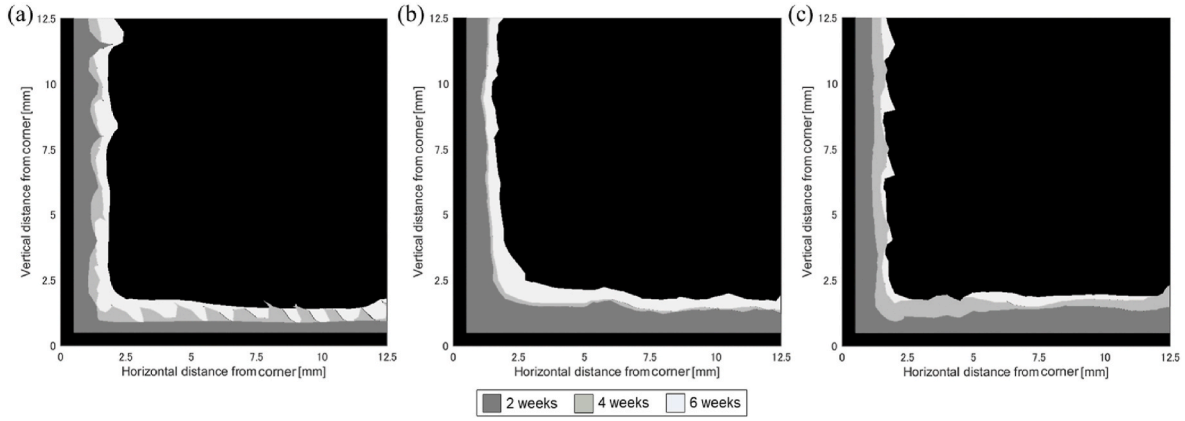

Fig. 17. Changes in the moisture-detected area with respect to the immersion time in the (a) acetone-degreased specimen, (b) hydrophilic-treated specimen, and (c) hydrophobic-treated specimen with an adhesive thickness of 0.1 mm.

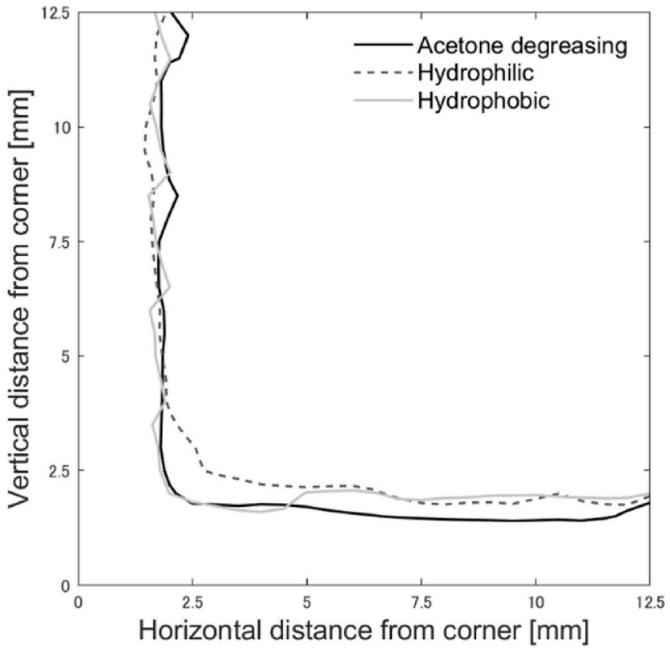

Fig. 18. Comparison of the moisture-detected area in specimens subjected to different surface treatments at an immersion time of six weeks.

to exhibit a slightly faster diffusion at the corners than the other two surface-treated specimens. It is possible that a hydrophilic surface, possessing relatively large surface energy compared to two other specimens, would influence on pulling of the moisture diffusion front due to interfacial tension [10]. Furthermore, the rapid moisture diffusion near the interface formed a measurable moisture content that diffused back toward the dry bulk direction, resulting in a broader moisture distribution compared to other specimens. This diffusion is expected to have a greater effect at the corner where the two diffusion axes intersect, and this effect is believed to be reflected in the experimental results.

By comparing the in-plane distributions of the specimens fabricated on substrates with different surface conditions, we could reaffirm that the moisture penetration rates were different in the cases of bulk diffusion and near-interface diffusion. In addition, the potential influence of substrate wettability on moisture diffusion, particularly in the diagonal direction, could be confirmed. However, the effect of substrate wettability on moisture diffusion remains unclear. Further study, such as the development of a direct measurement system for the moisture distribution in the thickness direction can enhance our understanding of moisture diffusion in the adhesive layer.

4. Conclusions

In summary, we investigated the effects of the adhesive thickness and surface wettability of various surface-treated substrates affect moisture penetration into the adhesive layer. We compared in-plane moisture

distributions using NIRS. First, we performed a numerical simulation using FEM with the diffusion coefficient obtained by fitting Fickian diffusion to the gravimetric changes of the bulk material. Results differed between experimental and numerical data for quartz–aluminum specimens, suggesting other factors influenced moisture diffusion beyond the diffusion coefficient. Conversely, quartz–quartz specimen results showed a relatively strong agreement with FEM results based on Fickian diffusion. Next, we compared the moisture distributions with two different adhesive thicknesses (0.1 and 0.3 mm) sandwiched by two quartz glass plates.

It is difficult to detect small amounts of moisture near the interface using NIRS because of the weak absorbance. Nevertheless, our experimental results showed that the diffusion coefficient of the adhesive layer, particularly the thinner layer, was approximately 1.6 times higher than that of the adhesive itself. This implies that the rapid penetration of moisture near the interface accelerated the moisture diffusion in the adhesive layer, particularly in the thin adhesive layers. Next, we compared the moisture distributions in a 0.1 mm-thick adhesive under different surface conditions. The hydrophilic-treated specimen showed a slightly different diffusion behavior than the specimens subjected to the hydrophobic and acetone degreasing treatments. This effect was particularly noticeable at the corners due to the penetration of moisture from multiple directions possibly resulting in a wider moisture distribution in the hydrophilic-treated specimen than in the others. By comparing the in-plane distributions of the specimens fabricated with substrates under different surface conditions, we confirmed again that the moisture penetration rates between bulk diffusion and near-interface diffusion were different. However, further research is required to better understand the effect of surface conditions on moisture diffusion. Further studies, such as the development of a direct measurement system in the thickness direction, could enhance our understanding of moisture diffusion in the adhesive layer.

Funding information

This research was funded by New Energy and Industrial Technology Development Organization (NEDO) under Project Number JPNP14014.

CRediT authorship contribution statement

Jin-Woo Han: Data curation, Formal analysis, Investigation, Methodology, Software, Validation, Visualization, Writing – original draft. **Yu Sekiguchi:** Conceptualization, Data curation, Project administration, Supervision, Validation, Writing – review & editing. **Kazumasa Shimamoto:** Methodology, Validation, Writing – review & editing. **Haruhisa Akiyama:** Conceptualization, Methodology, Validation, Writing – review & editing. **Chiaki Sato:** Conceptualization, Project administration, Supervision.

Declaration of competing interest

The authors declare that they have no known competing financial interests or personal relationships that could have appeared to influence the work reported in this paper.

Data availability

Data will be made available on request.

Acknowledgement

This work is based on the results of a completed project commissioned by the New Energy and Industrial Technology Development Organization (NEDO). We received support from AGC Co. Ltd. after the completion of the project. We would like to thank all the organizations for their support. We also thank Dr. Hiroshi Sasaki of Toagosei Co., Ltd. for suggesting the topic treated in this paper.

References

[1] Cavezza F, Boehm M, Terryn H, Hauffman T. A review on adhesively bonded aluminium joints in the automotive industry. Metals 2020;10:730. https://doi.org/10.3390/met10060730.
[2] Viana G, Costa M, Banea MD, da Silva LFM. A review on the temperature and moisture degradation of adhesive joints. Proc Inst Mech Eng : J Mater Des Appl 2017;231:488–501. https://doi.org/10.1177/1464420716671503.
[3] Houjou K, Shimamoto K, Akiyama H, Sato C. Effect of cyclic moisture absorption/desorption on the strength of epoxy adhesive joints and moisture diffusion coefficient. J Adhes 2022;98:1535–51. https://doi.org/10.1080/00218464.2021.1926242.
[4] Mubashar A, Ashcroft IA, Critchlow GW, Crocombe AD. Moisture absorption–desorption effects in adhesive joints. Int J Adhesion Adhes 2009;29:751–60. https://doi.org/10.1016/j.ijadhadh.2009.05.001.
[5] Han X, Crocombe AD, Anwar SNR, Hu P. The strength prediction of adhesive single lap joints exposed to long term loading in a hostile environment. Int J Adhesion Adhes 2014;55:1–11. https://doi.org/10.1016/j.ijadhadh.2014.06.013.
[6] Kim H-S, Huh J, Ryu J. Investigation of moisture-induced delamination failure in a semiconductor package via multi-scale mechanics. J Phys D Appl Phys 2011;44:034007. https://doi.org/10.1088/0022-3727/44/3/034007.
[7] Borges CSP, Marques EAS, Carbas RJC, Ueffing C, Weißgraeber P, da Silva LFM. Review on the effect of moisture and contamination on the interfacial properties of adhesive joints. Proc Inst Mech Eng C: J Mech Eng Sci 2021;235:527–49. https://doi.org/10.1177/0954406220944208.
[8] Adams RD, Cawley P. A review of defect types and nondestructive testing techniques for composites and bonded joints. NDT Int 1988;21:208–22. https://doi.org/10.1016/0308-9126(88)90333-1.
[9] Liljedahl CDM, Crocombe AD, Wahab MA, Ashcroft IA. Modelling the environmental degradation of adhesively bonded aluminium and composite joints using a CZM approach. Int J Adhesion Adhes 2007;27:505–18. https://doi.org/10.1016/j.ijadhadh.2006.09.015.
[10] Zanni-Deffarges MP, Shanahan MER. Diffusion of water into an epoxy adhesive: comparison between bulk behaviour and adhesive joints. Int J Adhesion Adhes 1995;15:137–42. https://doi.org/10.1016/0143-7496(95)91624-F.
[11] Houjou K, Shimamoto K, Akiyama H, Terasaki N, Sato C. Calculation of the moisture diffusion coefficient at the adhesive interface of double cantilever beam specimens by studying the fracture surfaces. Polym Test 2023;125:108141. https://doi.org/10.1016/j.polymertesting.2023.108141.
[12] Wapner K, Grundmeier G. Spatially resolved measurements of the diffusion of water in a model adhesive/silicon lap joint using FTIR-transmission-microscopy. Int J Adhesion Adhes 2004;24:193–200. https://doi.org/10.1016/j.ijadhadh.2003.09.008.
[13] Han J-W, Sekiguchi Y, Shimamoto K, Akiyama H, Sato C. Experimental measurement of moisture distribution in the adhesive layer using near-infrared spectroscopy. J Appl Polym Sci 2023;140:e53982. https://doi.org/10.1002/app.53982.
[14] Sugiman S, Salman S, Maryudi M. Effects of volume fraction on water uptake and tensile properties of epoxy filled with inorganic fillers having different reactivity to water. Mater Today Commun 2020;24:101360. https://doi.org/10.1016/j.mtcomm.2020.101360.
[15] Farris S, Pozzoli S, Biagioni P, Duó L, Mancinelli S, Piergiovanni L. The fundamentals of flame treatment for the surface activation of polyolefin polymers - a review. Polymer 2010;51:3591–605. https://doi.org/10.1016/j.polymer.2010.05.036.
[16] Drelich J, Chibowski E, Meng DD, Terpilowski K. Hydrophilic and superhydrophilic surfaces and materials. Soft Matter 2011;7:9804–28. https://doi.org/10.1039/C1SM05849E.
[17] Torniainen J, Afara IO, Prakash M, Sarin JK, Stenroth L, Töyräs J. Open-source python module for automated preprocessing of near infrared spectroscopic data. Anal Chim Acta 2020;1108:1–9. https://doi.org/10.1016/j.aca.2020.02.030.
[18] Christy AA. New insights into the surface functionalities and adsorption evolution of water molecules on silica gel surface: a study by second derivative near infrared spectroscopy. Vib Spectrosc 2010;51:42–9. https://doi.org/10.1016/j.vibspec.2010.06.003.
[19] Placette MD, Fan X, Zhao J-H, Edwards D. Dual stage modeling of moisture absorption and desorption in epoxy mold compounds. Microelectron Reliab 2012;52:1401–8. https://doi.org/10.1016/j.microrel.2012.03.008.
[20] Viana G, Costa M, Banea MD, da Silva LFM. Behaviour of environmentally degraded epoxy adhesives as a function of temperature. J Adhes 2017;93:95–112. https://doi.org/10.1080/00218464.2016.1179118.
[21] Le Guen-Geffroy A, Le Gac P-Y, Diakhate M, Habert B, Davies P. Long-term durability of CFRP under fatigue loading for marine applications. MATEC Web Conf 2018;165:07001. https://doi.org/10.1051/matecconf/201816507001.
[22] Wapner K, Stratmann M, Grundmeier G. In situ infrared spectroscopic and scanning Kelvin probe measurements of water and ion transport at polymer/metal interfaces. Electrochim Acta 2006;51:3303–15. https://doi.org/10.1016/j.electacta.2005.09.024.
[23] Swadener JG, Liechti KM, de Lozanne AL. The intrinsic toughness and adhesion mechanisms of a glass/epoxy interface. J Mech Phys Solid 1999;47:223–58. https://doi.org/10.1016/S0022-5096(98)00084-2.

[24] Vanlandingham MR, Eduljee RF, Gillespie Jr JW. Moisture diffusion in epoxy systems. J Appl Polym Sci 1999;71:787–98. https://doi.org/10.1002/(SICI)1097-4628(19990131)71:5<787::AID-APP12>3.0.CO;2-798.
[25] Katsivalis I, Feih S. Prediction of moisture diffusion and failure in glass/steel adhesive joints. Glass Struct Eng 2022;18:381–97. https://doi.org/10.1007/s40940-022-00194-w.
[26] Katsivalis I, Thomsen OT, Feih S, Achintha M. Effect of elevated temperatures and humidity on glass/steel adhesive joints. Int J Adhesion Adhes 2020;102:102691. https://doi.org/10.1016/j.ijadhadh.2020.102691.